

Search for $\psi(3770) \rightarrow$ charmless final states involving η or π^0 mesons

The BES Collaboration

M. Ablikim¹, L. An⁴, J.Z. Bai¹, Y. Bai¹, Y. Ban¹¹, X. Cai¹, H.F. Chen¹⁵, H.S. Chen¹, H.X. Chen¹, J.C. Chen¹, J. Chen¹, X.D. Chen⁵, Y.B. Chen¹, Y.P. Chu¹, Y.S. Dai¹⁷, Z.Y. Deng¹, S.X. Du^{1,18}, J. Fang¹, C.D. Fu¹, C.S. Gao¹, Y.N. Gao¹⁴, S.D. Gu¹, Y.T. Gu⁴, Y.N. Guo¹, K.L. He¹, M. He¹², Y.K. Heng¹, H.M. Hu¹, T. Hu¹, G.S. Huang^{1,19}, X.T. Huang¹², Y.P. Huang¹, X.B. Ji¹, L.L. Jiang¹, X.S. Jiang¹, J.B. Jiao¹², D.P. Jin¹, S. Jin¹, G. Li¹, H.B. Li¹, J. Li¹, L. Li¹, R.Y. Li¹, W.D. Li¹, W.G. Li¹, X.L. Li¹, X.N. Li¹, X.Q. Li¹⁰, Y.F. Liang¹³, B.J. Liu^{1,20}, C.X. Liu¹, Fang Liu¹, Feng Liu⁶, H.M. Liu¹, J.P. Liu¹⁶, H.B. Liu^{4,21}, J. Liu¹, R.G. Liu¹, S. Liu⁸, Z.A. Liu¹, F. Lu¹, G.R. Lu⁵, J.G. Lu¹, C.L. Luo⁹, F.C. Ma⁸, H.L. Ma¹, Q.M. Ma¹, M.Q.A. Malik¹, Z.P. Mao¹, X.H. Mo¹, J. Nie¹, R.G. Ping¹, N.D. Qi¹, J.F. Qiu¹, G. Rong¹, X.D. Ruan⁴, L.Y. Shan¹, L. Shang¹, X.Y. Shen¹, H.Y. Sheng¹, H.S. Sun¹, S.S. Sun¹, Y.Z. Sun¹, Z.J. Sun¹, X. Tang¹, J.P. Tian¹⁴, G.L. Tong¹, X. Wan¹, L. Wang¹, L.L. Wang¹, L.S. Wang¹, P. Wang¹, P.L. Wang¹, Y.F. Wang¹, Z. Wang¹, Z.Y. Wang¹, C.L. Wei¹, D.H. Wei³, N. Wu¹, X.M. Xia¹, G.F. Xu¹, X.P. Xu⁶, Y. Xu¹⁰, M.L. Yan¹⁵, H.X. Yang¹, M. Yang¹, Y.X. Yang³, M.H. Ye², Y.X. Ye¹⁵, C.X. Yu¹⁰, C.Z. Yuan¹, Y. Yuan¹, Y. Zeng⁷, B.X. Zhang¹, B.Y. Zhang¹, C.C. Zhang¹, D.H. Zhang¹, H.Q. Zhang¹, H.Y. Zhang¹, J.W. Zhang¹, J.Y. Zhang¹, X.Y. Zhang¹², Y.Y. Zhang¹³, Z.X. Zhang¹¹, Z.P. Zhang¹⁵, D.X. Zhao¹, J.W. Zhao¹, M.G. Zhao¹, P.P. Zhao¹, B. Zheng¹, H.Q. Zheng¹¹, J.P. Zheng¹, Z.P. Zheng¹, B. Zhong⁹, L. Zhou¹, K.J. Zhu¹, Q.M. Zhu¹, X.W. Zhu¹, Y.S. Zhu¹, Z.A. Zhu¹, Z.L. Zhu³, B.A. Zhuang¹, B.S. Zou¹

¹Institute of High Energy Physics, Beijing 100049, People's Republic of China

²China Center for Advanced Science and Technology (CCAST), Beijing 100080, People's Republic of China

³Guangxi Normal University, Guilin 541004, People's Republic of China

⁴Guangxi University, Nanning 530004, People's Republic of China

⁵Henan Normal University, Xinxiang 453002, People's Republic of China

⁶Huazhong Normal University, Wuhan 430079, People's Republic of China

⁷Hunan University, Changsha 410082, People's Republic of China

⁸Liaoning University, Shenyang 110036, People's Republic of China

⁹Nanjing Normal University, Nanjing 210097, People's Republic of China

¹⁰Nankai University, Tianjin 300071, People's Republic of China

¹¹Peking University, Beijing 100871, People's Republic of China

¹²Shandong University, Jinan 250100, People's Republic of China

¹³Sichuan University, Chengdu 610064, People's Republic of China

¹⁴Tsinghua University, Beijing 100084, People's Republic of China

¹⁵University of Science and Technology of China, Hefei 230026, People's Republic of China

¹⁶Wuhan University, Wuhan 430072, People's Republic of China

¹⁷Zhejiang University, Hangzhou 310028, People's Republic of China

¹⁸Present address: Zhengzhou University, Zhengzhou 450001, People's Republic of China

¹⁹Present address: University of Oklahoma, Norman, OK 73019, USA

²⁰Present address: University of Hong Kong, Pok Fu Lam Road, Hong Kong, Hong Kong

²¹Present address: Graduate University of Chinese Academy of Sciences, Beijing 100049, People's Republic of China

Received: 1 October 2009 / Revised: 31 December 2009 / Published online: 21 January 2010

© Springer-Verlag / Società Italiana di Fisica 2010

Abstract We search for $\psi(3770) \rightarrow \pi^+ \pi^- \eta$, $K^+ K^- \eta$, $p \bar{p} \eta$, $\rho^0 \pi^+ \pi^- \eta$, $K^+ K^- \pi^+ \pi^- \eta$, $p \bar{p} \pi^+ \pi^- \eta$, $p \bar{p} K^+ K^- \eta$ and $p \bar{p} K^+ K^- \pi^0$ using data samples of 17.3 and 6.5 pb^{-1} integrated luminosities recorded at the center-of-mass energies of 3.773 and 3.65 GeV, respectively, by the BES-II

detector operating at the BEPC collider. We obtain cross section measurements at both energies and upper limits on $\psi(3770)$ decay branching fractions to the final states studied.

1 Introduction

The $\psi(3770)$ has been thoroughly studied. It is popularly interpreted as a mixture of D -wave and S -wave of a $c\bar{c}$ bound state [1]. Since it lies just above the open charm pair $D\bar{D}$ threshold but below $\bar{D}D^*$ threshold, it was thought to almost entirely decay into $D\bar{D}$ meson pairs [2]. Under the assumption that there is only one single $\psi(3770)$ resonance in the energy range from 3.70 to 3.89 GeV, the BES Collaboration measured the branching fraction for $\psi(3770) \rightarrow$ non- $D\bar{D}$ decays to be $(14.7 \pm 3.2)\%$ [3–7]. So far, however, the sum of the exclusive non- $D\bar{D}$ decay branching fractions measured by both the BES and CLEO Collaborations remains to be less than 2% [8–21]. The anomalously large branching fraction for $\psi(3770) \rightarrow$ non- $D\bar{D}$ decays indicates that, either the conventional knowledge about the $\psi(3770)$ production and decays may need to be improved, or there are new structures or new dynamics effects at the considered energies [22, 23], or there may exist other exclusive non- $D\bar{D}$ decays of the $\psi(3770)$ not yet detected. In experiments, it is important to investigate more exclusive light hadron processes produced in e^+e^- annihilation at and off the $\psi(3770)$ resonance peak. By comparing the measured cross sections at and off the $\psi(3770)$ resonance peak, one may derive some helpful information about the non- $D\bar{D}$ decays of $\psi(3770)$.

In this paper, we report experimental studies of the charmless processes $e^+e^- \rightarrow \pi^+\pi^-\eta$, $K^+K^-\eta$, $p\bar{p}\eta$, $\rho^0\pi^+\pi^-\eta$, $K^+K^-\pi^+\pi^-\eta$, $p\bar{p}\pi^+\pi^-\eta$, $p\bar{p}K^+K^-\eta$ and $p\bar{p}K^+K^-\pi^0$ at $\sqrt{s} = 3.773$ and 3.65 GeV.

2 The BES-II detector

BES-II is a conventional cylindrical magnetic detector [24, 25] operated at the Beijing Electron-Positron Collider (BEPC). A 12-layer vertex chamber (VC) surrounding the beryllium beam pipe provides input to the event trigger, as well as coordinate information. A forty-layer main drift chamber (MDC) located just outside the VC yields precise measurements of charged particle trajectories with a solid angle coverage of 85% of 4π ; it also provides ionization energy loss (dE/dx) measurements which are used for particle identification. Momentum resolution of $1.7\%\sqrt{1+p^2}$ (p in GeV/c) and dE/dx resolution of 8.5% for Bhabha scattering electrons are obtained for the data taken at $\sqrt{s} = 3.773$ GeV. An array of 48 scintillation counters surrounding the MDC measures the time of flight (TOF) of charged particles with a resolution of about 180 ps for electrons. Outside the TOF, a 12 radiation length, lead-gas barrel shower counter (BSC), operating in limited streamer mode, measures the energies of electrons and photons over 80% of the total solid angle with an energy resolution of

$\sigma_E/E = 0.22/\sqrt{E}$ (E in GeV) and spatial resolutions of $\sigma_\phi = 7.9$ mrad and $\sigma_z = 2.3$ cm for electrons. A solenoidal magnet outside the BSC provides a 0.4 T magnetic field in the central tracking region of the detector. Three double-layer muon counters instrument the magnet flux return and serve to identify muons with momentum greater than 0.5 GeV/c . They cover 68% of the total solid angle.

3 Data and Monte Carlo

The analyzed data samples correspond to 17.3 pb^{-1} and 6.5 pb^{-1} integrated luminosities, which were collected at $\sqrt{s} = 3.773$ and 3.65 GeV, respectively, with the BES-II detector at the BEPC collider. These data samples were taken during 2001 and 2003. Throughout this paper we denote the two data sets the $\psi(3770)$ and the continuum data, respectively.

For the determination of the detection efficiency and the estimation of the background, we generate Monte Carlo events of $e^+e^- \rightarrow$ *exclusive light hadrons* by using a phase space generator based on the Monte Carlo simulation for the BES-II detector [26]. The generator, which was used in previous analyses [10–15], includes initial state radiation (ISR) and photon vacuum polarization corrections [27] with $1/s$ cross section energy dependence. The generator also includes final state radiation [28], decreasing the detection efficiency by less than 0.5%.

4 Analysis

To select candidate events for the processes $e^+e^- \rightarrow \pi^+\pi^-\eta$, $K^+K^-\eta$, $p\bar{p}\eta$, $\rho^0\pi^+\pi^-\eta$, $K^+K^-\pi^+\pi^-\eta$, $p\bar{p}\pi^+\pi^-\eta$, $p\bar{p}K^+K^-\eta$ and $p\bar{p}K^+K^-\pi^0$, we reconstruct the π^0 , η and ρ^0 particles through the decays $\pi^0 \rightarrow \gamma\gamma$, $\eta \rightarrow \gamma\gamma$ and $\rho^0 \rightarrow \pi^+\pi^-$, respectively.

4.1 Criteria of event selection

For the event selection, we require that there are at least two or four charged tracks in each event. All charged tracks used in this analysis are required to be well reconstructed in the MDC with good helix fits. They are required to be within $|\cos\theta| < 0.85$, where θ is the polar angle with respect to the beam axis, and to originate from the interaction region $\sqrt{V_x^2 + V_y^2} < 2.0 \text{ cm}$ and $|V_z| < 20.0 \text{ cm}$, where, V_x , V_y and V_z are the x , y and z coordinates of the point of the closest approach of the charged track relative to the beam axis. For each charged track, the combined dE/dx and TOF measurements are used to calculate the χ^2 ($= \chi_{dE/dx}^2 + \chi_{\text{TOF}}^2$) values and the corresponding confidence levels for the hypotheses that the particle is a pion, kaon, or proton (CL_π ,

CL_K and CL_p). If the combined confidence level CL_π for a pion hypothesis is greater than 0.001, it is identified as a pion. If the combined confidence level CL_K for a kaon hypothesis is greater than the combined confidence level CL_π for a pion hypothesis, it is identified as a kaon. If the combined confidence level CL_p for a proton hypothesis satisfies $CL_p/(CL_\pi + CL_K + CL_p) > 0.6$, it is identified as a proton.

For each process, there are two photons in the final state. To select the photons, we use the BSC measurement information. A neutral cluster is considered a good photon if it satisfies the following selection criteria. The energy of the cluster deposited in the BSC is greater than 50 MeV, the electromagnetic shower starts in the first five readout layers, the opening angle between the cluster and the nearest charged track is greater than 22° [29–32] and the opening angle between the cluster development direction and the photon emission direction is less than 37° [29–32].

In order to improve track momentum resolution and suppress background, we perform an energy-momentum conservation kinematic fit on each accepted charged and neutral track combination. Those combinations are retained if the χ^2 probability of the fit is greater than 0.01. For each process, it is likely that there are more than one combination satisfying the above selection criteria in each event. In this case we choose the combination with the largest χ^2 probability.

For the final states $\pi^+\pi^-\eta$ and $K^+K^-\eta$, to veto the background events from the process $\psi(3686) \rightarrow J/\psi\eta$ with $J/\psi \rightarrow \mu^+\mu^-$ or $J/\psi \rightarrow e^+e^-$, which are produced via initial state radiative return, we require that the invariant masses of the $\pi^+\pi^-$ and K^+K^- combinations be less than $3.0 \text{ GeV}/c^2$, respectively. To suppress background events from the process $e^+e^- \rightarrow (\gamma)e^+e^-$, we require that the sum of the energies deposited in the BSC of the two charged tracks should be less than 1.1 GeV . To remove background events from the process $e^+e^- \rightarrow (\gamma)\mu^+\mu^-$, we require that at least one of the two charged tracks be within $|\cos\theta| < 0.68$ and have momentum greater than $0.5 \text{ GeV}/c$, but it must not be identified as muon [9]. To study the process $e^+e^- \rightarrow \rho^0\pi^+\pi^-\eta$, we calculate the $\pi^+\pi^-$ invariant masses $M_{\pi^+\pi^-}$ of the selected $\pi^+\pi^-\pi^+\pi^-\gamma\gamma$ events, with the fitted momentum vectors from the kinematic fit. The mass window of $|M_{\pi^+\pi^-} - 0.7755| < 0.15 \text{ GeV}/c^2$ is taken as the ρ^0 signal region.

4.2 Candidate events observed from the data

The $\gamma\gamma$ invariant masses $M_{\gamma\gamma}$ of the selected $\pi^+\pi^-\gamma\gamma$, $K^+K^-\gamma\gamma$, $p\bar{p}\gamma\gamma$, $\pi^+\pi^-\pi^+\pi^-\gamma\gamma$, $K^+K^-\pi^+\pi^-\gamma\gamma$, $p\bar{p}\pi^+\pi^-\gamma\gamma$ and $p\bar{p}K^+K^-\gamma\gamma$ candidates are calculated with the fitted momentum vectors from the kinematic fit. Figures 1 and 2 show the $\gamma\gamma$ invariant masses for the candidate events of the processes studied. Using a Gaussian

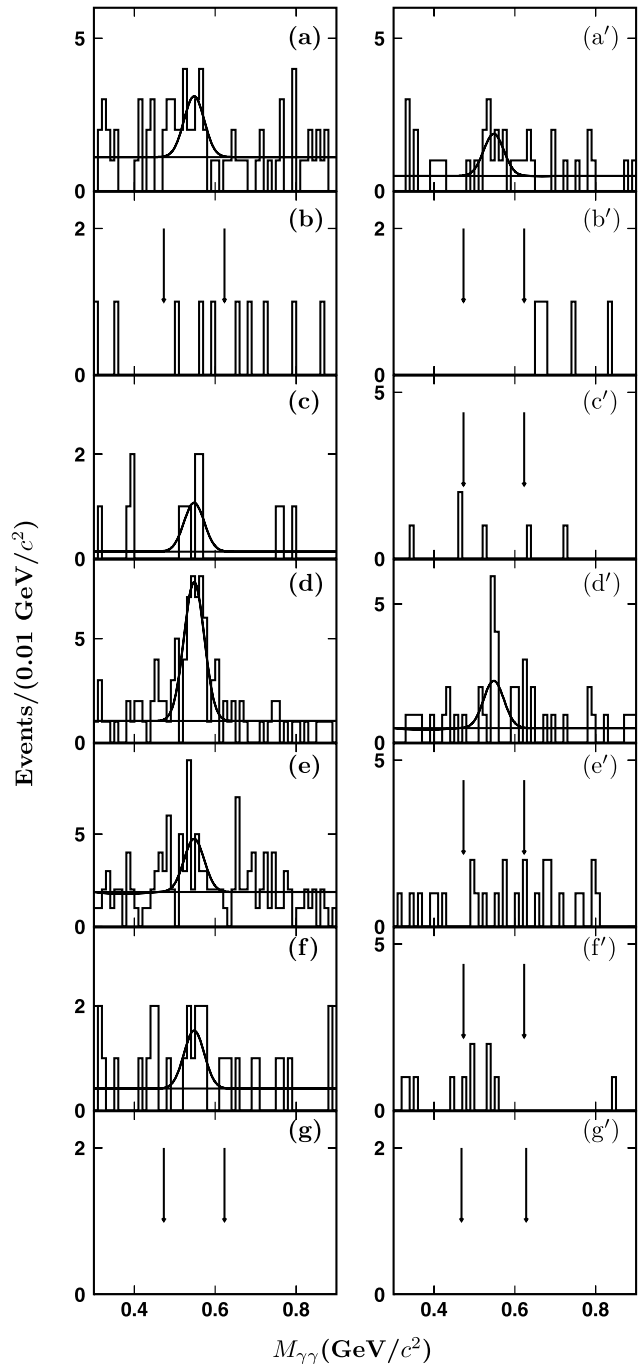


Fig. 1 Distributions of the $\gamma\gamma$ invariant masses for the selected combinations of $e^+e^- \rightarrow$ (a) $\pi^+\pi^-\gamma\gamma$, (b) $K^+K^-\gamma\gamma$, (c) $p\bar{p}\gamma\gamma$, (d) $\pi^+\pi^-\pi^+\pi^-\gamma\gamma$, (e) $K^+K^-\pi^+\pi^-\gamma\gamma$, (f) $p\bar{p}\pi^+\pi^-\gamma\gamma$ and (g) $p\bar{p}K^+K^-\gamma\gamma$ from the $\psi(3770)$ data (left) and the continuum data (right), where the pair of arrows denotes the η signal region

function to describe the η signal and a flat background, we fit the $\gamma\gamma$ invariant mass spectra in Figs. 1(a), (a'), (c), (d), (d'), (e) and (f). From the fits, we get the observed numbers N^{obs} of events from the data.

In Fig. 1(e') [(f')], no obvious η signal is observed. There are 10 (6) events in the η signal region, and 17 (5) events

outside the η signal region. By supposing that the distribution of the combinatorial $\gamma\gamma$ background is flat, 5.7 ± 1.4 (1.7 ± 0.7) background events are estimated in the η signal region. After background subtraction, we obtain 4.3 ± 3.4 (4.3 ± 2.6) events for $e^+e^- \rightarrow K^+K^-\pi^+\pi^-\eta$ ($p\bar{p}\pi^+\pi^-\eta$) observed from the continuum data. In the other figures, only a few events are observed. We obtain the numbers N^{obs} of

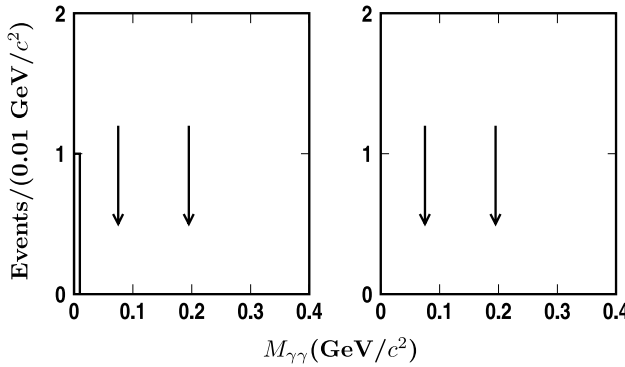


Fig. 2 Distributions of the $\gamma\gamma$ invariant masses for the selected combinations of $e^+e^- \rightarrow p\bar{p}K^+K^-\gamma\gamma$ from the $\psi(3770)$ data (left) and the continuum data (right), where the pair of arrows denotes the π^0 signal region

Table 1 Observed cross sections measured at $\sqrt{s} = 3.773$ GeV, where, N^{obs} is the observed number of events, N^b is the number of all the background events, N^{net} is the number of signal events, N^{up} is the upper limit on the number of events at 90% C.L., ϵ is the detection

$e^+e^- \rightarrow$	N^{obs}	N^b	N^{net} (or N^{up})	ϵ [%]	δ_{sys} [%]	σ (or σ^{up}) [pb]
$\pi^+\pi^-\eta$	12.5 ± 5.1	0.8 ± 0.6	11.7 ± 5.1	11.90 ± 0.17	11.5	$14.5 \pm 6.3 \pm 1.7$
$K^+K^-\eta$	3	–	<7.42	5.68 ± 0.11	8.9	<21.1
$p\bar{p}\eta$	5.8 ± 2.7	1.0 ± 0.2	4.8 ± 2.7	16.19 ± 0.19	11.0	$4.4 \pm 2.5 \pm 0.5$
$\rho^0\pi^+\pi^-\eta$	41.8 ± 7.6	0.4 ± 0.1	41.4 ± 7.6	4.83 ± 0.10	11.5	$126.0 \pm 23.1 \pm 14.5$
$K^+K^-\pi^+\pi^-\eta$	18.0 ± 6.3	1.9 ± 0.6	16.1 ± 6.3	3.76 ± 0.09	12.2	$63.0 \pm 24.6 \pm 7.7$
$p\bar{p}\pi^+\pi^-\eta$	6.9 ± 3.3	0.3 ± 0.0	6.6 ± 3.3	6.54 ± 0.12	13.0	$14.8 \pm 7.4 \pm 1.9$
$p\bar{p}K^+K^-\eta$	0	–	<2.44	0.88 ± 0.03	12.6	<46.6
$p\bar{p}K^+K^-\pi^0$	0	–	<2.44	1.99 ± 0.06	12.4	<8.2

Table 2 Observed cross sections measured at $\sqrt{s} = 3.65$ GeV, where, the symbols in this table have the same definitions as those in Table 1

$e^+e^- \rightarrow$	N^{obs}	N^b	N^{net} (or N^{up})	ϵ [%]	δ_{sys} [%]	σ (or σ^{up}) [pb]
$\pi^+\pi^-\eta$	8.6 ± 3.8	0.2 ± 0.2	8.4 ± 3.8	12.96 ± 0.17	10.1	$25.4 \pm 11.5 \pm 2.6$
$K^+K^-\eta$	0	–	<2.44	6.03 ± 0.11	8.9	<17.4
$p\bar{p}\eta$	1	–	<4.36	16.99 ± 0.19	8.3	<11.0
$\rho^0\pi^+\pi^-\eta$	10.7 ± 4.1	0.0 ± 0.0	10.7 ± 4.1	4.87 ± 0.10	11.5	$86.0 \pm 32.9 \pm 9.9$
$K^+K^-\pi^+\pi^-\eta$	4.3 ± 3.4	0.3 ± 0.3	4.0 ± 3.4	3.99 ± 0.09	13.5	$39.2 \pm 33.3 \pm 5.3$
$p\bar{p}\pi^+\pi^-\eta$	4.3 ± 2.6	0.0 ± 0.0	4.3 ± 2.6	6.39 ± 0.12	12.3	$26.3 \pm 15.9 \pm 3.2$
$p\bar{p}K^+K^-\eta$	0	–	<2.44	0.149 ± 0.007	13.0	<736.7
$p\bar{p}K^+K^-\pi^0$	0	–	<2.44	1.59 ± 0.04	12.4	<27.3

(see Ref. [10] for more details). The expected background abundances, N^b , are given in the third columns of Tables 1 and 2.

5 Observed cross sections

In this analysis we ignore possible interference between resonance and continuum production, and neglect the difference of the vacuum polarization corrections at $\sqrt{s} = 3.773$ and 3.65 GeV. The observed cross section for the process $e^+e^- \rightarrow f$ (f denotes a exclusive light hadron final state) can be determined by

$$\sigma_{e^+e^- \rightarrow f} = \frac{N^{\text{net}}}{\mathcal{L} \times \epsilon \times \mathcal{B}(\eta/\pi^0 \rightarrow \gamma\gamma)}, \quad (1)$$

where, N^{net} is the number of signal events for $e^+e^- \rightarrow f$, \mathcal{L} is the integrated luminosity of the data collected, ϵ is the efficiency for detection of the exclusive process, $\mathcal{B}(\eta/\pi^0 \rightarrow \gamma\gamma)$ is the branching fraction for $\eta/\pi^0 \rightarrow \gamma\gamma$.

The measured cross sections are quoted in the last columns of Tables 1 and 2, where the first error given is statistical and the second systematic. The latter error includes uncertainties in the integrated luminosity ($\sim 2.1\%$ [4]), the photon selection ($\sim 2.0\%$ per photon), the tracking efficiency ($\sim 2.0\%$ per track), the particle identification ($\sim 0.5\%$ per pion or kaon, $\sim 2.0\%$ per proton), the kinematic fit ($\sim 1.5\%$ [32]), the Monte Carlo statistics ($\sim [1.1\text{--}4.7]\%$), the background estimation ($\sim [0\text{--}7.0]\%$), the fit to the mass spectrum ($\sim [0\text{--}5.8]\%$), and the Monte Carlo modeling ($\sim 6.0\%$ [10]).

For other processes, however, only a few events are observed in the data. We set upper limits σ^{up} on their observed cross sections at 90% C.L., which are also quoted in the last columns of Tables 1 and 2. In this procedure, upper limits on

the observed numbers of events for these processes are set by using the Feldman-Cousins method [33] and neglecting background.

6 Upper limits on the observed cross section and the branching fraction for $\psi(3770) \rightarrow f$

Assuming that there are no other unknown structures and dynamics effects in addition to a single $\psi(3770)$ between 3.70 and 3.89 GeV, we can determine the observed cross section for $\psi(3770) \rightarrow f$ at $\sqrt{s} = 3.773$ GeV by

$$\sigma_{\psi(3770) \rightarrow f} = \sigma_{e^+e^- \rightarrow f}^{3.773 \text{ GeV}} - f_s \times \sigma_{e^+e^- \rightarrow f}^{3.65 \text{ GeV}}, \quad (2)$$

where, $\sigma_{e^+e^- \rightarrow f}^{3.773 \text{ GeV}}$ and $\sigma_{e^+e^- \rightarrow f}^{3.65 \text{ GeV}}$ are the observed cross sections for $e^+e^- \rightarrow f$ measured at $\sqrt{s} = 3.773$ and 3.65 GeV, respectively; f_s is the normalization factor for $1/s$ dependence of the cross section. The results on the numbers of $\sigma_{\psi(3770) \rightarrow f}$ for the final states $\pi^+\pi^-\eta$, $p\bar{p}\eta$, $\rho^0\pi^+\pi^-\eta$, $K^+K^-\pi^+\pi^-\eta$ and $p\bar{p}\pi^+\pi^-\eta$ are summarized in the second column of Table 3, where the first error is statistical, the second (third) energy-dependent (common) systematic error. The energy-dependent systematic uncertainty is from the uncertainties in the Monte Carlo statistics, the fit to the mass spectrum and the background estimation, while the common systematic uncertainty is from the other uncertainties.

For some final states, such as $K^+K^-\eta$, $p\bar{p}K^+K^-\eta$ and $p\bar{p}K^+K^-\pi^0$, no event is observed in the continuum data. Upper limit $\sigma_{\psi(3770) \rightarrow f}^{\text{up}}$ on the observed cross section for $\psi(3770) \rightarrow f$ is set by σ^{up} , which is upper limit on the observed cross section for $e^+e^- \rightarrow f$ at $\sqrt{s} = 3.773$ GeV set at 90% C.L. For other final states, however, $\sigma_{\psi(3770) \rightarrow f}^{\text{up}}$ is set under the Gaussian distribution hypothesis for $\sigma_{\psi(3770) \rightarrow f}$. These are quoted in the third column of Table 3.

Table 3 Upper limits $\mathcal{B}_{\psi(3770) \rightarrow f}^{\text{up}}$ on the branching fractions for $\psi(3770) \rightarrow f$ set at 90% C.L. In the table, $\sigma_{\psi(3770) \rightarrow f}$ is the observed cross section for $\psi(3770) \rightarrow f$, where the first error is the statistical, the second is the energy-dependent systematic error and the third is the common systematic error; $\sigma_{\psi(3770) \rightarrow f}^{\text{up}}$ is the upper

limit on $\sigma_{\psi(3770) \rightarrow f}$. For the processes $K^+K^-\eta$, $p\bar{p}K^+K^-\eta$ and $p\bar{p}K^+K^-\pi^0$, $\sigma_{\psi(3770) \rightarrow f}^{\text{up}}$ is set by the observed cross section upper limit σ^{up} for $e^+e^- \rightarrow f$ at $\sqrt{s} = 3.773$ GeV set at 90% C.L.; for the other processes, $\sigma_{\psi(3770) \rightarrow f}^{\text{up}}$ is set at 90% C.L. under a Gaussian distribution hypothesis

Decay mode	$\sigma_{\psi(3770) \rightarrow f}$ [pb]	$\sigma_{\psi(3770) \rightarrow f}^{\text{up}}$ [pb]	$\mathcal{B}_{\psi(3770) \rightarrow f}^{\text{up}}$ [$\times 10^{-3}$]
$\pi^+\pi^-\eta$	$-9.3 \pm 12.5 \pm 1.6 \pm 0.8$	<15.8	<2.3
$K^+K^-\eta$	–	<21.1	<3.1
$p\bar{p}\eta$	$4.4 \pm 2.5 \pm 0.3 \pm 0.4$	<7.7	<1.1
$\rho^0\pi^+\pi^-\eta$	$45.5 \pm 38.5 \pm 3.3 \pm 5.1$	<98.3	<14.5
$K^+K^-\pi^+\pi^-\eta$	$26.3 \pm 39.7 \pm 4.0 \pm 3.0$	<84.0	<12.4
$p\bar{p}\pi^+\pi^-\eta$	$-9.8 \pm 16.6 \pm 0.8 \pm 1.2$	<22.2	<3.3
$p\bar{p}K^+K^-\eta$	–	<46.6	<6.9
$p\bar{p}K^+K^-\pi^0$	–	<8.2	<1.2

The observed cross section for $\psi(3770)$ production at $\sqrt{s} = 3.773$ GeV was measured to be $\sigma_{\psi(3770)}^{\text{obs}} = (7.15 \pm 0.27 \pm 0.27)$ nb [3, 10, 34] by the BES Collaboration. Upper limit on the branching fraction for $\psi(3770) \rightarrow f$ can be determined by

$$\mathcal{B}_{\psi(3770) \rightarrow f}^{\text{up}} = \frac{\sigma_{\psi(3770) \rightarrow f}^{\text{up}}}{\sigma_{\psi(3770)}^{\text{obs}} \times (1 - \delta)}, \quad (3)$$

which are quoted in the last column of Table 3. Here, the δ is to consider the uncertainty of the measured $\sigma_{\psi(3770)}^{\text{obs}}$.

7 Summary

By analyzing the data samples of 17.3 and 6.5 pb^{-1} integrated luminosities taken at $\sqrt{s} = 3.773$ and 3.65 GeV with the BES-II detector at the BEPC collider, we derive cross sections or upper limits on cross sections for the processes $e^+e^- \rightarrow \pi^+\pi^-\eta, K^+K^-\eta, p\bar{p}\eta, \rho^0\pi^+\pi^-\eta, K^+K^-\pi^+\pi^-\eta, p\bar{p}\pi^+\pi^-\eta, p\bar{p}K^+K^-\eta$ and $p\bar{p}K^+K^-\pi^0$ at both energies. From these measurements, we extract upper limits on observed cross sections and branching fractions for $\psi(3770)$ decay into these final states at 90% C.L.

Acknowledgements The BES collaboration thanks the staff of BEPC for their hard efforts. This work is supported in part by the National Natural Science Foundation of China under contracts Nos. 10491300, 10225524, 10225525, 10425523, 10935007, the Chinese Academy of Sciences under contract No. KJ 95T-03, the 100 Talents Program of CAS under Contract Nos. U-11, U-24, U-25, the Knowledge Innovation Project of CAS under Contract Nos. U-602, U-34 (IHEP), the National Natural Science Foundation of China under Contract No. 10225522 (Tsinghua University). This work is also supported by Young Innovation Fund of IHEP (No. H95461E).

References

1. P.A. Rapidis et al. (MARK-I Collaboration), Phys. Rev. Lett. **39**, 526 (1978)
2. W. Bicino et al. (DELCO Collaboration), Phys. Rev. Lett. **40**, 671 (1978)
3. M. Ablikim et al. (BES Collaboration), Phys. Rev. Lett. **97**, 121801 (2006)
4. M. Ablikim et al. (BES Collaboration), Phys. Lett. B **641**, 145 (2006)
5. M. Ablikim et al. (BES Collaboration), Phys. Rev. D **76**, 122002 (2007)
6. M. Ablikim et al. (BES Collaboration), Phys. Lett. B **659**, 74 (2008)
7. C. Amsler et al. (Particle Data Group), Phys. Lett. B **667**, 1 (2008)
8. J.Z. Bai et al. (BES Collaboration), High Energy Phys. Nucl. Phys. **28**(4), 325 (2004)
9. J.Z. Bai et al. (BES Collaboration), Phys. Lett. B **605**, 63 (2005)
10. M. Ablikim et al. (BES Collaboration), Phys. Lett. B **650**, 111 (2007)
11. M. Ablikim et al. (BES Collaboration), Phys. Lett. B **656**, 30 (2007)
12. M. Ablikim et al. (BES Collaboration), Eur. Phys. J. C **52**, 805 (2007)
13. M. Ablikim et al. (BES Collaboration), Phys. Lett. B **670**, 179 (2008)
14. M. Ablikim et al. (BES Collaboration), Phys. Lett. B **670**, 184 (2008)
15. M. Ablikim et al. (BES Collaboration), Eur. Phys. J. C **64**, 243 (2009)
16. N.E. Adam et al. (CLEO Collaboration), Phys. Rev. Lett. **96**, 082004 (2006)
17. T.E. Coans et al. (CLEO Collaboration), Phys. Rev. Lett. **96**, 182002 (2006)
18. B.A. Briere et al. (CLEO Collaboration), Phys. Rev. D **74**, 031106 (2006)
19. D. Cronin-Hennessy et al. (CLEO Collaboration), Phys. Rev. D **74**, 012005 (2006)
20. G.S. Huang et al. (CLEO Collaboration), Phys. Rev. Lett. **96**, 032003 (2006)
21. G.S. Adams et al. (CLEO Collaboration), Phys. Rev. D **73**, 012002 (2006)
22. M. Ablikim et al. (BES Collaboration), Phys. Rev. Lett. **101**, 102004 (2008)
23. M. Ablikim et al. (BES Collaboration), Phys. Lett. B **668**, 263 (2008)
24. J.Z. Bai et al. (BES Collaboration), Nucl. Instrum. Methods A **344**, 319 (1994)
25. J.Z. Bai et al. (BES Collaboration), Nucl. Instrum. Methods A **458**, 627 (2001)
26. M. Ablikim et al. (BES Collaboration), Nucl. Instrum. Methods A **552**, 344 (2005)
27. E.A. Kuraev, V.S. Fadin, Yad. Fiz. **41**, 733 (1985)
28. E. Barberio, Z. Wąs, Comput. Phys. Commun. **79**, 291 (1994)
29. M. Ablikim et al. (BES Collaboration), Phys. Lett. B **597**, 39 (2004)
30. M. Ablikim et al. (BES Collaboration), Phys. Lett. B **603**, 130 (2004)
31. M. Ablikim et al. (BES Collaboration), Phys. Lett. B **608**, 24 (2005)
32. M. Ablikim et al. (BES Collaboration), Nucl. Phys. B **727**, 395 (2005)
33. G.J. Feldman, R.D. Cousins, Phys. Rev. D **57**, 3873 (1998)
34. M. Ablikim et al. (BES Collaboration), Phys. Lett. B **652**, 238 (2007)